Post-print of: Camargo-Ramírez, R., Val-Torregrosa, B. and San Segundo, B. “MiR858-mediated regulation of flavonoid-specific MYB transcription factor genes controls resistance to pathogen infection in Arabidopsis" in Plant and cell physiology (Ed. Oxford University Press), vol. 59, issue 1 (Jan. 2018), p. 190-204. The final versión is available at DOI 10.1093/pcp/pcx175

MiR858-Mediated Regulation of Flavonoid-Specific MYB Transcription Factor genes Controls Resistance to Pathogen Infection in Arabidopsis

Running head: **Arabidopsis miR858 modulates disease resistance**

Corresponding author: Blanca San Segundo

Subject Area: Environmental and stress responses

Black and white figures: 2 (Figs 3, 5)
Colour figures: 5 (Figs 1, 2, 4, 6, 7)
Tables: 0
Type and number of supplementary material: Supplementary figures (10 Figures) and Supplementary Table (1 Table)

MiR858-Mediated Regulation of Flavonoid-Specific MYB Transcription Factor Genes Controls Resistance to Pathogen Infection in Arabidopsis

Rosany Camargo-Ramírez[1], Beatriz Val-Torregrosa[1] and Blanca San Segundo[1,2,*]

[1]Centre for Research in Agricultural Genomics (CRAG) CSIC-IRTA-UAB-UB. Campus Universitat Autònoma de Barcelona (UAB), Bellaterra (Cerdanyola del Vallés), 08193 Barcelona, Spain. [2]Consejo Superior de Investigaciones Científicas (CSIC), Barcelona, Spain.

* Corresponding autor:
E-mail, blanca.sansegundo@cragenomica.es; Fax, 34 93 5636601

Running Head: Arabidopsis miR858 modulates disease resistance.

Abbreviations: ABA, abscisic acid; CAD, cinnamyl-alcohol dehydrogenase; CaMV, Cauliflower mosaic virus; C4H, Cinnamate-4-hydroxylase; CHI, Chalcone isomerase; CHS, Chalcone synthase; 4CL, 4-Coumarate-CoA Ligase; DPBA, diphenylboric acid 2-amino-ethyester; dpi, days post-inoculation; ET, ethylene; ETI, Effector triggered immunity; F3H, Flavonol-3-hydroxylase; F3'H, Flavonol-3'-hydroxylase; FLS, Flavonol synthase; GUS, β-glucoronidase; JA, jasmonic acid; miRNA, microRNA; hpi, hours post-inoculation; MYB, V-myb myeloblastosis viral oncogene homolog; PAL, phenylalanine ammonia-lyase; PAMP, pathogen-associated molecular patterns; PRR, pattern recognition receptor; PTI, pathogen-triggered immunity; RT-qPCR, reverse transcription-quantitative PCR; ROS, reactive oxygen species; SA, salicylic acid; TIR1, transport inhibitor response.

Abstract

MicroRNAs (miRNAs) are a class of short endogenous non-coding small RNAs that direct post-transcriptional gene silencing in eukaryotes. In plants, the expression of a large number of miRNAs has been shown to be regulated during pathogen infection. However, the functional role of the majority of these pathogen-regulated miRNAs has not been elucidated. In this work, we investigated the role of Arabidopsis miR858 in the defense response of Arabidopsis plants to infection by fungal pathogens with necrotrophic (*Plectosphaerella cucumerina*) or hemibiotrophic (*Fusarium oxysporum* and *Colletotrichum higginsianum*) lifestyles. Whereas overexpression of *MIR858* enhances susceptibility to pathogen infection, interference with miR858 activity by target mimics (*MIM858* plants) results in disease resistance. Upon pathogen challenge, stronger activation of the defense genes *PDF1.2* and *PR4* occurs in *MIM858* plants than in wild-type plants, whereas pathogen infection induced weaker activation of these genes in *MIR858* overexpressor plants. Reduced miR858 activity, and concomitant up-regulation of miR858 target genes, in *MIM858* plants, also leads to accumulation of flavonoids in Arabidopsis leaves. The antifungal activity of phenylpropanoid compounds, including flavonoids, is presented. Furthermore, pathogen infection or treatment with fungal elicitors is accompanied by a gradual decrease in *MIR858* expression in wild-type plants, suggesting that miR858 plays a role in PAMP (Pathogen-associated molecular patterns)-triggered immunity. These data support that miR858 is a negative regulator of Arabidopsis immunity and provide new insights into the relevant role of miR858-mediated regulation of the phenylpropanoid biosynthetic pathway in controlling Arabidopsis immunity.

Keywords: *Arabidopsis thaliana*, *Colletotrichum higginsianum*, defense response, *Fusarium oxysporum*, miR858, *Plectosphaerella cucumerina*.

Introduction

As sessile organisms, plants have evolved multiple mechanisms to perceive and efficiently respond to potential pathogens which involve extensive transcriptional reprogramming of defense gene expression. Immunity is initiated by the recognition of microbial molecular signatures, collectively named pathogen-associated molecular patterns (PAMPs), by host pattern recognition receptors (PRRs) (Boller and He 2009; Jones and Dangl 2006; Zipfel 2014). Sensing PAMPs triggers a general defense response referred to as PAMP-triggered immunity (PTI), which operates against most pathogens (Bigeard et al. 2015). Among others, PTI components include production of reactive oxygen species (ROS), reinforcement of cell wall by deposition of lignin, activation of protein phosphorylation/dephosphorylation processes, and accumulation of antimicrobial compounds (e.g. phytoalexins). The induction of a group of genes known collectively as *Pathogenesis-Related* (*PR*) genes is also a ubiquitous response of plants to pathogen infection (van Loon et al. 2006). To counteract this innate defense, pathogens can deliver virulence effector proteins into plant cells that suppress PTI (Boller and He 2009). In turn, many plants have evolved Resistance (R) proteins that directly or indirectly detect microbial effectors. This recognition triggers a rapid and effective host defense response, the so called effector-triggered immunity (ETI), which is highly specific (isolate-, race- or pathovar-specific) (Cui et al. 2015). Treatment with microbial elicitors triggers the same responses that are observed in infected tissues (Boller and Felix 2009). Immune responses against fungal and bacterial pathogens have been traditionally considered as protein-based defense mechanisms, largely independent from the RNA-based mechanisms that typically operate in antiviral defense. The phytohormones salicylic acid (SA), jasmonic acid (JA), and ethylene (ET) function as key signaling molecules in disease resistance in plants (Denance et al. 2013; Glazebrook 2005). JA and ET might act synergistically or antagonistically in regulating plant defense against pathogen infection, whereas ET/JA and SA signaling pathways often interact in an antagonistic manner.

MicroRNAs (miRNAs) are a class of small noncoding RNAs that direct post-transcriptional gene silencing through sequence-specific cleavage or translational repression of target mRNAs (Brodersen et al. 2008; Llave et al. 2002). The crucial role of miRNAs in diverse plant developmental processes, such as leaf, flower and root development, hormone signaling and responses to abiotic stress is well documented (e.g. drought, salinity, cold, heat, oxidative stress and nutrient deficiency) (Chen 2009; Chiou et al. 2006; Jeong and Green 2013; Mallory et al. 2004; Palatnik et al. 2003). Increasing evidence also supports that miRNAs play a role in the plant response to pathogen infection (Borges and Martienssen 2015; Campo et al. 2013; Staiger et al. 2013; Weiberg et al. 2014). The first evidence for miRNAs affecting pathogen defense came from *A. thaliana*, where treatment with the flagellin-derived elicitor peptide flg22 from *Pseudomonas syringae* causes an increase in miR393, a negative regulator of TIR1/AFB auxin receptors. The miR393-mediated repression of auxin signaling enhances resistance to bacterial pathogens (Navarro et al. 2006). However, although a substantial fraction of the miRNA transcriptome has been shown to be responsive to pathogen infection in different plant species, the exact role of most of these pathogen-regulated miRNAs in plant immunity remains elusive. Our current knowledge on distinct miRNAs involved in disease resistance comes mainly from studies in Arabidopsis plants infected with the bacterial pathogen *P. syringae*, and less is known about miRNAs mediating resistance against fungal pathogens.

On the other hand, the general phenylpropanoid pathway metabolism is known to produce an enormous array of secondary metabolites that fulfill many vital biological functions during plant development and responses to

environmental cues (e.g UV protection, defense responses against insect herbivory, flower coloring, auxin transport inhibition) (Falcone Ferreyra et al. 2012; Naoumkina et al. 2010). The phenylpropanoid pathway is required for the biosynthesis of flavonoids and monolignols, the building blocks of lignin. In Arabidopsis, distinct members of the MYB (V-myb myeloblastosis viral oncogene homolog) family of transcription factors function as transcriptional activators of genes involved in flavonoid biosynthesis, namely the *AtMYB11*, *AtMYB12*, and *AtMYB111* genes (Liu et al. 2015; Mehrtens et al. 2005; Stracke et al. 2007). It is also known that miR858 targets, and cleaves, *AtMYB11*, *AtMYB12* and *AtMYB111* transcripts (Addo-Quaye et al. 2008; Dubos et al. 2010; Fahlgren et al. 2007; Sharma et al. 2016).

In this study, we investigated the potential role of miR858 in Arabidopsis disease resistance. Transgenic plants overexpressing *MIR858* were found to be more susceptible to infection by fungal pathogens whereas interference with miR858 activity by the target mimic strategy (*MIM858* lines) confers pathogen resistance. Fungal pathogens with a necrotrophic (*Plectosphaerella cucumerina*) or hemibiotrophic (*Colletotrichum higginsianum*, *Fusarium oxysporum* f. sp. *conglutinans*) lifestyle were assayed in this work. Resistance to pathogen infection in *MIM858* plants is associated to a stronger induction of ET-mediated defense responses and flavonoid accumulation, but not lignification. The antifungal activity of flavonoids (e.g. naringenin, kaempferol) and the phenylpropanoid p-coumaric acid is presented. Overall, results here presented support that miR858 functions as a negative regulator of Arabidopsis immunity by controlling accumulation of antifungal phenylpropanoid compounds.

Results

Increased susceptibility to infection by fungal pathogens in Arabidopsis plants overexpressing *MIR858*

In *A. thaliana*, miR858 is encoded by two loci, *MIR858A* and *MIR858B*. Mature miRNAs, miR858a and miR858b, are 21 nucleotides in length and differ in the last nucleotide, at both the 5' and the 3' end (miR858a, 5'-uuucguugucuguucgaccuu-3'; miR858b, 5'-uucguugucuguucgaccuug-3'). To investigate whether miR858 plays a role in Arabidopsis immunity, we overexpressed either *MIR858A* or *MIR858B* under the control of the *CaMV35S* promoter (hereafter *MIR858A* OE and *MIR858B* OE plants, respectively). Control Arabidopsis plants carrying the empty vector were also produced. The transgenic Arabidopsis lines overexpressing a *MIR858* gene accumulated higher levels of the corresponding pre- and mature miR858 sequences (**Supplementary Fig. S1A)**. No phenotypic differences were observed between *MIR858* overexpressor and control plants as determined by visual inspection (**Supplementary Fig. S1B**) and number of rosette leaves (**Supplementary Fig. S1C**).

The *MIR858* overexpressor plants were tested for resistance to infection by the fungus *P. cucumerina*. The Arabidopsis/*P. cucumerina* pathosystem is a well-established model for studies on basal resistance to necrotrophic fungi (Llorente et al. 2005). This fungus causes sudden death and blight in different crop species (i.e. melon, soybean, snap bean, pumpkin, squash, zucchini, or white luppine), and also infects *A. thaliana*. As controls, *agb1.2* (impaired in the heterotrimeric G-protein β-subunit) and *lin1* (impaired in the expression of the high affinity nitrate transporter 2.1, *NRT2.1*) mutant plants were always included in disease resistance assays against *P. cucumerina*. The *agb1.2* mutant has been shown to exhibit enhanced susceptibility to *P. cucumerina* (Llorente et al. 2005), whereas *lin1* displays resistance to this fungus (Gamir et al. 2014). Of interest, *MIR858A*

and *MIR858B* overexpressor plants displayed enhanced susceptibility to infection by *P. cucumerina* compared to control plants (wild-type and empty vector) (**Fig. 1A)**. As expected, *lin1* and *agb1.2* plants showed resistance and susceptibility, respectively, to infection by this pathogen (**Fig. 1A**). Trypan blue staining of *P. cucumerina*-inoculated leaves confirmed extensive fungal colonization in *MIR858* OE plants whereas, under the same experimental conditions, a few hyphae were observed on leaves of control plants (**Fig. 1B**). Susceptibility to fungal infection in *MIR858* OE plants was corroborated by a decrease in survival of *P. cucumerina*-infected plants (**Fig. 1C**). Moreover, qPCR analysis confirmed increased levels of *P. cucumerina* DNA in leaves of *MIR858* OE plants compared to control plants (**Fig. 1D)**.

We also investigated whether *MIR858* overexpression enhances susceptibility to fungal pathogens with a hemibiotrophic lifestyle, such as *Colletotichum higginsianum*. This fungus is the causal agent of the anthracnose leaf spot disease on many cultivated forms of *Brassica* species, including *A. thaliana* (O'Connell et al. 2004). Interestingly, *MIR858* OE plants exhibited enhanced susceptibility to infection by *C. higginsianum* as revealed by visual inspection of disease symptoms, determination of plant survival and disease severity (percentage of diseased leaf area), and quantification of fungal biomass in the infected plants (**Fig. 1E-H**).

From these results, it is concluded that overexpression of *MIR858*, either *MIR858A* or *MIR858B*, increases susceptibility to infection by fungal pathogens with a necrotrophic (*P. cucumerina*) and hemibiotrophic (*C. higginsianum*) lifestyle in Arabidopsis.

Inactivation of miR858 activity by target mimics enhances resistance to infection by fungal pathogens

The use of transgenic plants designed to interfere with the activity of specific miRNAs through the target mimicry strategy (named as *MIM* plants) has proven to be a valuable resource to investigate miRNA function, including those involved in immunity (Soto-Suarez et al. 2017; Todesco et al. 2010). Target mimicry is an endogenous regulatory mechanism that plants use to negatively regulate the activity of specific miRNAs in which an endogenous long non-coding RNA (*IPS1*, *Induced by Phosphate Starvation1*) binds to miR399, but the pairing is interrupted by a mismatched loop at the expected miRNA cleavage site that abolishes the cleavage effect (Franco-Zorrilla et al. 2007). In this way, *IPS1* serves as a decoy for miR399 to interfere with the binding of this miRNA to its target transcripts leading to miRNA degradation.

In this work, Arabidopsis *MIM858* plants were examined for pathogen resistance (for details on the production of *MIM858* plants, see Todesco et al. 2010). Although to a different extent, the accumulation of mature miR858a and miR858b sequences was significantly reduced in *MIM858* plants compared to control wild-type and transgenic empty vector plants (**Supplementary Fig. S2A**). The *MIM858* plants showed normal phenotype as judged by estimation of rosette leaf number and diameter (**Supplementary Fig. S2B, C**). Most importantly, *MIM858* plants exhibited enhanced resistance to *P. cucumerina* infection (**Fig. 2A**; **Supplementary Fig. S3**). Depending on the line, 56-88% of the *MIM858* plants survived at 15 dpi, but only 21% of the wild-type and 28% of the empty vector plants survived (**Fig. 2B**). Trypan blue staining of infected leaves revealed limited fungal growth in *MIM858* and control *lin1* plants, whereas the fungus extensively proliferated in the inoculated leaves of wild-type, empty vector and *agb1.2* plants (**Fig. 2C**). qPCR analysis also revealed reduced fungal biomass in *MIM858* plants compared to control plants (**Fig. 2D**).

MIM858 plants exhibited resistance to infection by *C. higginsianum* (**Fig. 2E-H**). In agreement with visual inspection of the fungal-infected plants, *MIR858* plants that have been infected with *C. higginsianum* showed higher survival rates, reduced percentage of diseased leaf area and less fungal biomass relative to control plants (wild-type and empty vector) (**Fig. 2E-H**). The resistance phenotype of *MIM858* plants to *P. cucumerina* and *C. higginsianum* infection is consistent with the phenotype of susceptibility that is observed in plants overexpressing *MIR858*.

During the course of this work, we also examined whether interference with miR858 activity confers resistance *Fusarium oxysporum* f. sp. *conglutinans* (*FOC*), a hemibiotrophic pathogen that causes wilt disease on a broad range of plant species, including *A. thaliana* (Mauch-Mani and Slusarenko 1994; O'Connell et al. 2004). Upon pathogen challenge, chlorosis and leaf curling was evident in control plants (wild-type, empty vector), culminating in yellowing and necrosis, whereas *MIM858* lines exhibited much milder symptoms (**Supplementary Fig. S4A)**. The *FOC*-inoculated *MIM858* plants exhibited higher survival and reduced diseased leaf area as well as less fungal biomass in their leaves compared to control plants (**Supplementary Fig. S4B-D**).

Collectively, disease resistance assays demonstrated that *MIR858* overexpression increases susceptibility to infection by fungal pathogens, whereas interference with miR858 activity results in enhanced resistance to pathogen infection. These findings are consistent with a role of miR858 in regulating resistance to pathogen infection.

Moreover, we examined the expression of the defense-related genes *PDF1.2* and *PR4* in *MIM858* and *MIR858* overexpressor plants. As expected, infection with *P. cucumerina* induced the expression of these genes in wild type plants (**Fig. 3**). To note, *PDF1.2* and *PR4* expression was induced at a much higher level in fungal-infected *MIM858* plants compared to fungal-infected wild-type plants (**Fig. 3A**). In the literature there are many examples of resistance to pathogen infection in Arabidopsis with enhanced *PDF1.2* expression, including resistance to *P. cucumerina* (Berrocal-Lobo et al. 2002; Coego et al. 2005). Contrary to this, *P. cucumerina* infection induced weaker activation of *PDF1.2* and *PR4* expression in *MIR858* overexpressor plants compared to wild-type plants (**Fig. 3B**). We did not observe important differences in pathogen responsiveness of *VSP2*, *LOX2*, *PR1a* and *NPR1* expression between *MIM858* plants and *MIR858* overexpressor plants (**Supplementary Fig. S5**). As *PDF1.2* and *PR4* expression is known to be regulated by the defense-related hormone ethylene, the observation that *MIM858* plants respond to pathogen infection with a super-induction of *PDF1.2* and *PR4* expression, while these genes are weakly induced in *MIR858* overexpressor plants, raises the possibility that miR858 is a negative regulator of ethylene-dependent signaling. FutIure research is needed to test whether interference with miR858 activity and/or *MIR858* overexpression has an effect on ethylene signaling pathways in Arabidopsis immunity.

MIR858 expression is down-regulated during fungal infection and treatment with fungal elicitors

To gather further support for the involvement of miR858 in Arabidopsis immunity, we examined the accumulation of miR858a and miR858b precursor sequences (pre-miR858a and pre-miR-858b) in wild-type plants during infection with *P. cucumerina*. A down-regulation of *MIR858* expression was observed during the entire period of infection here examined (24, 48 and 72 hours post-inoculation) (**Fig. 4A, left panel**). The observed reduction in the accumulation of miR858 precursor transcripts in response to pathogen infection

correlated well with a decrease in the accumulation of the corresponding mature miR858 sequences (**Fig. 4A, left panel**). Similarly, miR858 accumulation (precursor and mature sequences) decreased in Arabidopsis plants that have been treated with a crude preparation of elicitors obtained by autoclaving and sonicating *P. cucumerina* mycelium (**Fig. 4B**). Thus, not only pathogen infection, but also treatment with fungal elicitors results in down-regulation of *MIR858* expression suggesting a role of miR858 in PTI.

We investigated whether the reduced level of miR858 accumulation in fungal-infected plants was the consequence of a reduced activity of the *MIR858* promoter. Towards this end, we generated transgenic plants expressing the *ß-glucuronidase* (*GUS*) reporter gene under the control of the *MIR858A* promoter (*promMIR858A::GUS*). The *promMIR858A::GUS* plants were inoculated with *P. cucumerina* spores, or mock inoculated. GUS activity was monitored by histochemical (**Fig. 4C**) and quantitative fluorimetric analysis (**Supplementary Fig. S6**). The *MIR858A* promoter was found to be active in rosette leaves of mock-inoculated Arabidopsis plants, its activity being maintained during the entire experimental period (**Fig. 4C, left panel**). In contrast, a remarkable decrease in *MIR858A* promoter activity occurred in the *P. cucumerina*-inoculated *promMIR858A::GUS* plants that was not observed in the control *prom35SCaMV::GUS* plants (**Fig. 4C; Supplementary Fig. S6**). These results indicated that *MIR858A* expression is transcriptionally repressed during *P. cucumerina* infection.

Resistance to *P. cucumerina* infection in *MIM858* plants relies on the accumulation of phenylpropanoid compounds with antifungal activity

A miR858-guided cleavage of transcripts encoding distinct members of the large family of MYB transcription factors is well documented. The miR858 target genes are: *AtMYB11*, *AtMYB12*, *AtMYB13*, *AtMYB20* and *AtMYB111* (Addo-Quaye et al. 2008; Fahlgren et al. 2007; Sharma et al. 2016). Among them, *AtMYB11*, *AtMYB12* and *AtMYB111* are known to be involved in the biosynthesis of phytoalexins (Dubos et al. 2010). Although several other *MYB* genes are predicted to be target genes for miR858, their validation as miR858 targets is still lacking. We confirmed that *MIM858* plants accumulate higher levels of miR858 targeted-transcripts than wild-type caused by mimicry-triggered miR858 degradation (**Supplementary Figure S7A**). We also confirmed down-regulation of the miR858-targeted genes involved in phytoalexin biosynthesis in *MIR858* overexpressor lines (e.g *AtMYB11*, *AtMYB12*, *AtMYB111*) (**Supplementary Figure S7B**). These results indicated that expression of the flavonoid-specific *AtMYB11*, *AtMYB12*, *AtMYB111* genes is up-regulated and down-regulated in *MIM858* plants and *MIR858* overexpressor plants, respectively. Furthermore, we observed that expression of *AtMYB11*, *AtMYB12* and *AtMYB111* is up-regulated by *P. cucumerina* infection in wild-type plants (**Supplementary Fig. S7C**), which is consistent with the observed down-regulation of *MIR858* expression in *P. cucumerina*-infected wild-type plants (see **Fig. 4A**). Regarding the function of the miR858 target genes *AtMYB11*, *AtMYB12* and *AtMYB111*, these transcription factors are known to function as activators of genes involved in the production of flavonols from 4-coumaroyl-CoA, namely *Chalcone synthase* (*CHS*), *Chalcone Isomerase* (*CHI*), *Flavonol-3-hydroxylase* (*F3H*) and *Flavonol Synthase1* (*FLS1*) (Liu et al. 2015; Mehrtens et al. 2005; Stracke et al. 2007). Here it is worth mentioning that, with the exception of flavonol synthase, genes involved in the central pathway for flavonoid biosynthesis in Arabidopsis are mostly single-copy genes. Consistent with the observed up-regulation of flavonoid-specific *MYB* transcription factors in *MIM858* plants, metabolome analysis revealed accumulation of flavonoids in these plants (Sharma et al. 2016).

Phenylalanine serves as the precursor for the production of 4-coumaroyl-CoA, which is the precursor molecule for the flavonoid and lignin branches of the general phenylpropanoid pathway. We speculated that miR858-mediated alterations of *AtMYB11*, *AtMYB12* and *AtMYB111* expression in *MIM858* plants could have an impact on the expression of genes in the general phenylpropanoid pathway, beyond the steps in which the miR858-targeted genes function. To test this possibility, we examined the expression of genes acting upstream of the flavonoid branch in the general phenylpropanoid pathway, that is, genes involved in the production of p-coumaril-CoA from phenylalanine. They were: *PAL* (*phenylalanine ammonia-lyase*), *C4H* (*cinnamate-4-hydroxilase*) and *4CL* (*4-Coumarate-CoA-ligase*). Regarding *PAL* genes, up to four *PAL* genes have been identified in the Arabidopsis genome (*PAL1*, *PAL2*, *PAL3* and *PAL4*). Expression analyses revealed up-regulation of *PAL4*, *C4H* and *4CL* in *MIM858* plants, whereas their expression was down-regulated in *MIR858* overexpressor plants (**Fig. 5A, B**). As for the other *PAL* genes, *PAL1* and *PAL 3* were down-regulated, but *PAL2* expression was not affected, in *MIM858* plants (**Supplementary Fig. S9A**). *PAL1*, *PAL2* and *PAL3* expression was not significantly affected in *MIR858A* overexpressor plants (**Supplementary Fig. S9B**). These findings indicate that, in addition to the miR858-targeted *MYB* genes functioning in the flavonoid branch of the phenylpropanoid pathway, genes acting upstream of the flavonoid-specific pathway (e.g. *PAL4*, *C4H* and *4CL*) are also regulated in *MIM858* and *MIR858* overexpressor plants. Thus, interference with miR858 activity in *MIM858* plants has consequences that go beyond alterations in flavonoid-specific *MYB* genes (*AtMYB11, AtMYB12, AtMYB111*) in the general phenylpropanoid biosynthetic pathway.

Next, we investigated whether phenylpropanoid compounds, in particular flavonoids, are relevant in conferring disease resistance in *MIM858* plants. For this, we examined flavonoid accumulation in leaves of wild-type, *MIM858* and *MIR858A* OE plants that have been inoculated with *P. cucumerina* spores, or mock-inoculated. DPBA (diphenylboric acid 2-aminoethyl ester) staining was used to visualize flavonoid accumulation. DPBA binds to flavonoids and fluoresces *in vivo,* and the flavonoid-DPBA conjugates have unique fluorescent color (e.g. yellow-green fluorescence correspond to DPBA bound to the flavonol kaempferol) (Peer et al. 2001). Microscopic analysis of DPBA-stained leaves revealed clear differences in flavonoid accumulation between *MIM858* and wild-type plants. Under non-infection conditions, only a few tiny green-fluorescence signals were distinguishable on the leaf surface of wild type plants. In *MIM858* plants, however, larger regions showing intense green-yellow fluorescence were consistently observed under non-infection conditions (**Fig. 6A**). The green-yellow fluorescence of flavonoid-DPBA conjugates that is observed in *MIM858* plants might well reveal kaempferol-DPBA conjugates, as previously reported (Peer et al. 2001). In favor of this possibility, a metabolomic analysis of *MIM858* plants revealed that kaempferol was the most abundant flavonoid accumulating in these plants (Sharma et al. 2016).

Importantly, whereas the flavonoid-DPBA fluorescence localized at restricted areas in leaves of mock-inoculated plants, the fluorescence exhibited a more generalized distribution in *P. cucumerina*-infected leaves (**Fig. 6A**). This generalized pattern of fluorescence was observed in fungal-infected wild-type and fungal-infected *MIM858* plants. Plants overexpressing *MIR858A* did not show accumulation of flavonoid-DPBA fluorescence, either under control or under infection conditions (**Fig. 6A**).

We then hypothesized that the increased levels of flavonoids accumulating in *MIM858* plants might be responsible of the phenotype of disease resistance that is observed in these plants. In this work, we investigated the possible antifungal activity of the flavonoids naringenin and kaempferol, as well as the phenylpropanoid p-

coumaric acid. The two flavonoids (kaempferol and naringenin) were found to be effective for inhibition of *P. cucumerina* growth, the later one having a greater antifungal activity (**Fig. 6B)**. The phenylpropanoid p-coumaric acid was, however, more effective for inhibition of *P. cucumerina* growth than each one of the flavonoids (naringenin, kaempferol) (**Fig. 6B**). After 48 hours of incubation, a concentration of 1 mM of p-coumaric acid results in 55% inhibition of *P. cucumerina* growth (45% growth of control cultures). Increasing the concentration of p-coumaric acid did not significantly increase the antifungal potency of this compound. Equally, when increasing the concentration of naringenin above 2 mM (or kaempherol above 4 mM), their antifungal activity did not further increase. These findings indicate that the potency of these compounds against *P. cucumerina* might have reached maximum values under the experimental conditions here assayed. Finally, microscopical observations of fungal cultures revealed alterations in the morphology of hyphae in cultures that have been grown in the presence of one or another compound. Hyphae with constricted regions were frequently observed in treated-cultures compared the control cultures (**Supplementary Fig. S9**). These findings suggest that accumulation of phenylpropanoid compounds exhibiting antifungal activity, such as kaempferol, naringenin and p-coumaric acid, might be responsible, at least in part, of the disease resistance phenotype that is observed in *MIM858* plants.

Pathogen resistance in *MIM858* plants does not requires lignification

It is generally assumed that lignification plays a role in resistance to pathogen infection (Miedes et al. 2014). Lignin is deposited in the secondary cell wall, thus, providing a physical barrier against pathogen invasion. However, the observation that *MIM858* plants had reduced lignification in vascular and interfascicular tissues (Sharma et al. 2016) prompted us to investigate whether resistance to *P. cucumerina* infection in *MIM858* plants depends on lignification.

Lignin accumulation was examined in mock-inoculated and *P. cucumerina*-inoculated wild-type, *MIM858* and *MIR858A* overexpressor plants using the whole-mount phloroglucinol staining method. In the absence of pathogen infection, lignin was detected in wild-type, but not in *MIM858* plants (**Fig. 7, upper panels**). Also, the expression of the lignin-specific *CAD* (cinnamyl alcohol dehydrogenase) genes (*CAD5*, *CAD6*) involved in the synthesis of the immediate precursors of lignin was found to be down-regulated in *MIM858* plants compared to wild-type plants (**Supplementary Fig. S10**). Lignin accumulation greatly increased in response to fungal infection in wild-type plants, but not in *MIM858* plants (**Fig. 7, lower panels)**. Finally, lignin accumulation in *MIR858A* plants was confirmed (**Fig. 7, right panels**).

From these results, it is concluded that lignification, most probably, does not contribute to pathogen resistance in *MIM858* plants. Down-regulation of miR858 and concomitant up-regulation of miR858 target genes appears to re-direct the metabolic flux towards the production of phenylpropanoid compounds, some of them exhibiting antifungal activity, away from lignin biosynthesis.

Discussion

In this study we provide evidence for the involvement of miR858 in Arabidopsis immunity. We show that overexpression of miR858 renders Arabidopsis plants more susceptible to pathogen infection, whereas inhibition of miR858 activity by target mimics results in enhanced resistance to infection by necrotrophic (*P. cucumerina*)

and hemibiotrophic (*F.oxysporum* f. sp. *conglutinans*, *C. higginsianum*) pathogens. These findings suggest that miR858 functions as a negative regulator of disease resistance in Arabidopsis. In wild type plants, *MIR858* expression is down-regulated not only during pathogen infection, but also in response to treatment with fungal elicitors, indicating that miR858 is a component of PTI. The increased resistance to fungal infection that is observed in *MIM858* plants is associated to a stronger induction of *PDF1.2*, *PR4* expression upon pathogen challenge. Enhanced disease susceptibility in *MIR858* overexpressor plants is also consistent with a lower expression of these defense-related genes during pathogen infection.

Interestingly, blocking miR858 activity by target mimics results in up-regulation of the flavonoid-specific target genes *AtMYB11*, *AtMYB12* and *AtMYB111*, as well as genes upstream of the flavonoid branch in the phenylpropanoid pathway (e.g. *PAL4*, *C4H* and *4CL*). Thus, *PAL4*, *C4H*, *4CL* and miR858-regulated *MYB* genes might be regulated in a coordinated manner in order to prioritize flavonoid production in *MIM858* plants. At present, however, it is not possible to determine whether alterations in the expression of phenylpropanoid genes in *MIM858* plants are due to a feed-back control by metabolite levels, or to protein-protein interactions with other regulatory proteins in transcriptional complexes controlling flavonoid biosynthesis. In this respect, enzymes involved in flavonoid biosynthesis have been proposed to form protein complexes, or metaboloms, to establish efficient metabolic flux of flavonoid biosynthesis (Waki et al. 2016).

Visualization of flavonoids in Arabidopsis leaves using DPBA staining revealed changes in the pattern of flavonoid accumulation between wild-type and plants with altered expression of *MIR858*. In particular, *MIM858* plants accumulated higher levels of flavonoids compared to wild-type plants, whereas flavonoids were barely detected in miR858 overexpressor plants. Furthermore, *P. cucumerina* infection induced flavonoid accumulation, the flavonoids showing a more widespread, generalized distribution in *P. cucumerina*-infected leaves than in mock-inoculated leaves. Given that flavonoids have been reported to be capable of long-distance movement in Arabidopsis (Buer et al. 2007), a widespread distribution of flavonoids in *P. cucumerina*-infected leaves points to a possible function of flavonoids as signaling molecules as part of the host defense response to pathogen infection. In other studies, flavonoids were proposed to function as signal molecules in auxin transport, or during symbiotic nitrogen fixation and mycorrhizal associations (Falcone Ferreyra et al. 2012).

Our data show that naringenin and kampherol, as well as p-coumaric acid, exhibit antifungal activity against *P. cucumerina.* Indeed, the antifungal potency of p-Coumaric acid was higher than that of the two flavonoids assayed in this work. Knowing that these compounds accumulate in leaves of *MIM858* plants (present work; Sharma et al. 2016), it is likely that their accumulation contributes to antifungal resistance. The *in vitro* antifungal activity of the individual phenylpropanoid compounds assayed in this work (p-coumaric acid, naringenin, kaempferol) is, however, weaker than that of known plant antimicrobial peptides, such as lipid transfer proteins or thionins (Molina et al. 1993a; Molina et al. 1993b). Resistance to infection in *MIM858* plants might well rely on the simultaneous action and/or combined effect of antifungal activities of phenylpropanoids, including flavonoids, rather than on the activity of individual compounds. Along with this, the expression of genes involved in flavonoid biosynthesis is induced in the interaction of plants with different pathogens, and certain flavonoids (or flavonoid-derivatives) isolated from plant tissues exhibited *in vitro* antimicrobial activity (Bollina et al. 2010; Dai et al. 1996; Galeotti et al. 2008). Concerning the mechanisms by which flavonoids exert their antifungal activity, it has been proposed that they function as ROS scavengers and chelators of metals that might generate ROS via de Fenton reaction. Potentially, flavonoids might act as antioxidant molecules in

protecting the plant cell from oxidative stress induced by environmental stress (Falcone Ferreyra et al. 2012). However, the relevance of the antioxidant properties for flavonoid in the plant response to pathogen infection is still a topic of debate.

Lignification has been associated with resistance to pathogen infection in different plant species. We show that sequestration of miR858 by target mimics in *MIM858* plants leads to a reduction in lignin accumulation and down-regulation of genes encoding the specific and last step enzyme for production of monolignols (*CAD5*, *CAD6*). Most importantly, no accumulation of lignin was observed in *P. cucumerina*-infected *MIM858* plants, supporting that resistance to fungal infection in these plants does not require a lignification response. These results also indicated that, at some level, miR858-guided regulation of flavonoid-specific *MYB* genes is involved in the cross-talk between the two phenylpropanoid branches for the production of flavonols or monolignols. Interference with miR858 activity would then re-direct the phenylpropanoid pathway towards the production of antifungal compounds, including flavonoids, at the cost of lignin synthesis. In previous studies, it was reported that flavonoids accumulate in cell walls during pathogen infection (Dai et al. 1996). It is then tempting to hypothesize that a reduced lignification in *MIM858* plants may facilitate the incorporation of flavonoids in host cell walls. Further studies are, however, needed to clarify this aspect.

Under our experimental conditions, *MIR858* overexpressor plants and *MIM858* plants grew and developed normally in the absence of pathogen infection. Differences in plant growth were, however, described in *MIR858* OE or *MIM858* plants compared with wild type plants (Sharma et al. 2016). A possible explanation for the different growth responses in *MIR858* OE and *MIM858* plants might be the photoperiod condition used to grow the plants. In our work, plants were always grown under neutral day condition (12h light/12h dark photoperiod), whereas (Sharma et al. 2016) grew plants under a long day photoperiod (16h light/8h dark photoperiod). A photoperiod-dependent regulation of *MIR858* expression was also described (Sharma et al. 2016). Further studies are needed to establish whether links between light regulation of *MIR858* expression and growth performance exists.

Collectivelly, the results presented here demonstrate that alterations on *MIR858* expression have important consequences in disease resistance, and that Arabidopsis plants adjust their general phenylpropanoid metabolism in order to prioritize the production of phenylpropanoid compounds having antifungal activities as an effective immune response. The fact that a single miRNA, such as miR858, can regulate the expression of multiple genes involved in a specific pathway, such as the phenylpropanoid pathway, would ensure proper production of antifungal compounds as part of the plant defense response which, in turn, would increase the plant's ability to cope with pathogen infection. From a more practical point of view, this course of study can provide new ways to develop strategies to increase disease resistance in plants through inhibition of miR858 activity. In other studies, miR828 and miR858 were reported to regulate the expression of *MYB2* gene homologs that function in Arabidopsis trichome formation and cotton fiber development, these particular miRNAs also being regulated during adaptation to high temperature in cotton (Guan et al. 2014). MiR858 was also reported to mediate tolerance to drought stress in the desert plant *Ammopiptanthus mongolicus* (Gao et al. 2016). Very recently, Piya et al. (2017) described that miR858 post-transcriptionally regulates *MYB83* during cyst nematode parasitism, a process in which miR858 and *MYB83* expression appear to be connected through a feedback circuit. Together, these observations point to a functional role of miR858 in different developmental processes and metabolism pathways, as well as during adaptation to biotic and abiotic stresses. Whether miR858 is a common component

of plant adaptive responses to different types of environmental stresses needs to be further investigated. The information provided in this work extends our knowledge on miRNAs involved in plant immunity while laying the foundation for future research to uncover links between phenylpropanoid metabolism and plant immunity.

Materials and Methods

Plant and fungal materials

Arabidopsis thaliana (ecotype Columbia-0) plants were grown under a 12h light/12h dark photoperiod and 60% relative humidity at a temperature of 22 ± 2°C. For *in vitro* assays, seeds were grown for 14 days on MS medium containing 0.8% agar and vitamins. The Arabidopsis mutants *agb1.2* (Llorente et al. 2005) and *lin1* (Gamir et al. 2014) were grown as described above.

Fungi were grown at 28ºC on PDA (potato dextrose agar) supplemented with chloramphenicol (34mg/ml). Spores were collected adding sterile water and adjusted to the desired concentration using a Neubauer counting chamber.

Generation of transgenic *Arabidopsis* plants

For *MIR858* overexpression, the DNA fragment containing the precursor sequence for each miR858 species was PCR amplified from genomic DNA using gene-specific primers (503 bp and 428 bp DNA fragments for the miR858a and miR858b precursor, respectively). Primers are listed in **Supplementary Table S1**. Precursor DNA sequences were cloned into the pCAMBIA1300 binary vector under the control of the *CaMV35S* (*Cauliflower Mosaic Virus 35S*) promoter.

To obtain the *MIR858Apromoter:GUS* construct, the DNA sequence of the *MIR858A* promoter region was extracted from NCBI (http://www.ncbi.nlm.nih.gov). The transcription start site was identified by using the transcription start site identification program for plants (http://linux1.softberry.com/). The DNA sequence covering 2 kb upstream of the transcription start site of *MIR858A* was PCR amplified from genomic DNA, and cloned into the pCAMBIA1391z plant binary vector. All PCR products were verified by sequencing. The plant expression vectors were transferred to the *Agrobacterium tumefaciens* strain GV3101. *Arabidopsis* (Col-0) plants were transformed using the floral dip method. Transgenic lines harboring the empty vector (pCAMBIA1300 or pCAMBIA1391z) were also obtained and used as controls.

Fungal infection and elicitor treatment

Three-week-old *Arabidopsis* plants were spray-inoculated with a spore suspension of *P. cucumerina* at the appropriated concentration. In each case, at least three independent transgenic lines for each genotype were assayed (*MIR858A* OE or *MIR858B* OE, *MIM858* lines). As controls, wild-type and empty vector plants were assayed. The *agb1.2* (susceptible) and *lin1* (resistant) mutants were included in infection experiments with *P. cucumerina*. Infection assays with *F. oxysporum f. sp. conglutinans* (FOC) were performed by applying the spore suspension to the soil near the base of the plant (200 µl, 1 x 10^6 spores/ml). Inoculations with *C. higginsianum* were carried out by placing 2 drops of the spore suspension on each leaf. Infected plants, as well as mock-inoculated plants were maintained under high humidity for the required period of time. The progress of

disease symptoms was followed with time. Elicitor treatment was performed by spraying three-week old plants with an elicitor extract obtained from *P. cucumerina* (300 µg/ml) as described (Casacuberta et al. 1992). Three independent experiments (infection with fungal spores, treatment with fungal elicitors) were performed with at least 24 plants per genotype in each experiment. Statistically significant differences among genotypes were determined by one-way ANOVA test.

Lesion areas were quantified with the ASSESS v2.0 software on 4 inoculated leaves per plant (24 plants per genotype). Quantification of fungal DNA on infected leaves was carried out by real-time PCR using specific primers for the corresponding fungus and the Arabidopsis *UBIQUITIN21* (*At5g25760*) gene as an internal control (Soto-Suarez et al. 2017). PCR primers are listed in **Supplementary Table S1.**

For trypan blue staining, leaves were fixed by vacuum infiltration for 1h in ethanol:formaldehyde:acetic acid (80:3.5:5 v/v), stained with lactophenol blue solution for 4 h, washed with 70% ethanol for 5 min. Leaves were placed in glass slides with glycerol an observed using a Zeiss Axiophot microscope.

Expression analysis RT-qPCR and stem-loop RT-qPCR

Total RNA was extracted from rosette leaves using the TRIzol Reagent (Invitrogen). Reverse transcription reactions were performed using DNase-treated total RNA (1 µg) and reverse transcriptase (Applied Biosystems) and oligo-dT_{18} (Sigma, Aldrich). RT-qPCR (Reverse transcriptase quantitative PCR) was performed in optical 96-well plates in a Light Cycler 480 (Roche) using SYBR® Green. Primers were designed using Primer3 software (http://www.ncbi.nlm.nih.gov). The average cycle threshold (Ct) values were obtained by PCR from three independent biological replicates and normalized to the average Ct values for the *beta-tubulin2* gene from the same RNA preparations, yielding the ΔCt value or normalized expression (relative expression). The $2^{-\Delta\Delta Ct}$ method was used to analyze relative changes in gene expression or fold change (infected/elicitor-treated vs mock-inoculated) and visualized by log2 transformation. Primers used for RT-qPCR and stem-loop RT-PCR are listed in **Supplementary Table S1**. ANOVA tests were used to evaluate differences in gene expression.

Analysis of GUS activity

Histochemical staining of GUS enzyme activity was performed according to (Jefferson et al. 1987). Briefly, leaves were fixed by vacuum infiltration for 1h in ethanol:formaldehyde:acetic acid (80:3.5:5 v/v), stained with lactophenol blue solution for 4 hours, and washed with 70% ethanol (5 minutes). Leaves were placed in glass slides with glycerol an observed using a microscopy Aixophot DP70. Quantitative GUS activity assay was carried out using the fluorimetric substrate 4-methylumbelliferyl-β-D-glucoronide (MUG) at a final concentration of 1 mM.

Determination of lignin content

Lignin accumulation was determined by whole-mount fluoroglucinol staining. For this, the Arabidopsis seedlings were fixed on ethanol 70% for 24h, stained with phloroglucinol (0.012 mg/ml ethanol:HCl 50:50 v/v) for 2 min, and washed with water (5 min). Leaves were placed in glass slides with glycerol an observed on an Olympus DP71 microscope.

In vivo staining of flavonoids

Flavonoids were visualized *in vivo* by the fluorescence of flavonoid-conjugated DPBA (diphenylboric acid 2-amino-ethylester) following the protocol described by (Watkins et al. 2014) . Briefly, the leaves were excised and submerged in an aqueous solution containing 0.01% (v/v) Triton X-100 and 2.52 mg/ml DPBA for 2.5 hours. Leaves were then washed in deionized water for 1 min. Fluorescence was recorded on an AixoPhotDP70 microscope with excitation at 488 nm. The DPBA fluorescence emission was collected between 520 nm to 600 nm.

In vitro antifungal assays

The *in vitro* antifungal activity of naringenin, kaempferol and p-coumaric acid was determined by measuring the absorbance of fungal cultures at 595 nm in 96-well microtiter plates (Cavallarin et al. 1998). In microtiter plates, 150 µl of potato dextrose broth (PDB) medium containing chloramphenicol (0.03 µg/µl) were mixed with 50 µl of *P. cucumerina* spores (10^6 spores/ml). Spores were allowed to germinate for 6h. The secondary metabolite was then added to the desired final concentration. The microtiter plates were incubated at 25ºC for 48 hours and the absorbance was read (OD 595 nm). Fungal growth was also checked microscopically to confirm the spectrophotometric data. As a control, the antifungal agent nystatin was used (0.1mg/ml).

Funding

This work was supported by grants from the Spanish Ministry of Economy and Competitiveness [BIO2012-32838, BIO2015-67212-R] and by the CERCA Programme from the Generalitat de Catalunya. We acknowledge financial support from MINECO through the "Severo Ochoa Programme for Centres of Excellence in R&D" 2016-2019 [SEV-2015-0533]". R. Camargo was a recipient of a PhD grant from the "Ministerio de Educación, Cultura y Deportes (FPU12/02812). Beatriz Val Torregrosa received a PhD grant from the "Ministerio de Economia, Industria y Competitividad" (BES-2016-076289) .

Disclosures

The authors have no conflicts of interest to declare

Acknowledgements

We thank Drs Detlef Weigel and Ignacio Rubio-Somoza for providing the *MIM858* line. We are also thankful to Drs. Antonio Molina (Centro de Biotecnología y Genómica de Plantas, Madrid) for the *P. cucumerina* strain and *agb1.2* mutant, Richard O'Connell (Max Planck Institute for Plant Breeding Research, Köln, Germany) for *C. higginsianum*, Antonio di Pietro (Universidad de Córdoba) for *F. oxysporum* f. sp. *conglutinans*, Victor Flors (Universitat Jaume I, Castellón de la Plana) for the *lin1* mutant, Mauricio Soto (CRAG) for assistance in parts of this work, David Caparrós (CRAG) for helpful advice on lignin analysis and Sonia Campo for critical reading.

References

Addo-Quaye, C., Eshoo, T.W., Bartel, D.P. and Axtell, M.J. (2008) Endogenous siRNA and miRNA targets identified by sequencing of the Arabidopsis degradome. *Curr. Biol.* 18: 758-762.

Berrocal-Lobo, M., Molina, A. and Solano, R. (2002) Constitutive expression of ETHYLENE-RESPONSE-FACTOR1 in Arabidopsis confers resistance to several necrotrophic fungi. *Plant J.* 29: 23-32.

Bigeard, J., Colcombet, J. and Hirt, H. (2015) Signaling mechanisms in Pattern-Triggered Immunity (PTI). *Mol. Plant* 8: 521-539.

Boller, T. and Felix, G. (2009) A renaissance of elicitors: perception of Microbe-Associated Molecular Patterns and danger signals by Pattern-Recognition Receptors. *Annu. Rev. Plant Biol.* 60: 379-406.

Boller, T. and He, S.Y. (2009) Innate immunity in plants: an arms race between pattern recognition receptors in plants and effectors in microbial pathogens. *Science* 324: 742-744.

Bollina, V., Kumaraswamy, G.K., Kushalappa, A.C., Choo, T.M., Dion, Y., Rioux, S., et al. (2010) Mass spectrometry-based metabolomics application to identify quantitative resistance-related metabolites in barley against *Fusarium head blight*. *Mol. Plant Pathol.* 11: 769-782.

Borges, F. and Martienssen, R.A. (2015) The expanding world of small RNAs in plants. *Nat. Rev. Mol. Cell Biol.* 16: 727-741.

Brodersen, P., Sakvarelidze-Achard, L., Bruun-Rasmussen, M., Dunoyer, P., Yamamoto, Y.Y., Sieburth, L., et al. (2008) Widespread translational inhibition by plant miRNAs and siRNAs. *Science* 320: 1185-1190.

Buer, C.S., Muday, G.K. and Djordjevic, M.A. (2007) Flavonoids are differentially taken up and transported long distances in Arabidopsis. *Plant Physiol.* 145: 478-490.

Campo, S., Peris-Peris, C., Sire, C., Moreno, A.B., Donaire, L., Zytnicki, M., et al. (2013) Identification of a novel microRNA (miRNA) from rice that targets an alternatively spliced transcript of the *Nramp6* (*Natural resistance-associated macrophage protein 6*) gene involved in pathogen resistance. *New Phytol.* 199: 212-227.

Casacuberta, J.M., Raventos, D., Puigdomenech, P. and San Segundo, B. (1992) Expression of the gene encoding the PR-like protein *PRms* in germinating maize embryos. *Mol. Gen. Gen.* 234: 97-104.

Cavallarin, L., Andreu, D. and San Segundo, B. (1998) Cecropin A-derived peptides are potent inhibitors of fungal plant pathogens. *Mol. Plant Microbe Interact.* 11: 218-227.

Coego, A., Ramirez, V., Gil, M.J., Flors, V., Mauch-Mani, B. and Vera, P. (2005) An Arabidopsis homeodomain transcription factor, *OVEREXPRESSOR OF CATIONIC PEROXIDASE 3*, mediates resistance to infection by necrotrophic pathogens. *Plant Cell* 17: 2123-2137.

Cui, H., Tsuda, K. and Parker, J.E. (2015) Effector-Triggered Immunity: From pathogen perception to robust defense. *Ann. Rev. Plant Biol.* 66: 487-511.

Chen, X. (2009) Small RNAs and their roles in plant development. *Ann. Rev. Cell Dev. Biol.* 25: 21-44.

Chiou, T.J., Aung, K., Lin, S.I., Wu, C.C., Chiang, S.F. and Su, C.L. (2006) Regulation of phosphate homeostasis by MicroRNA in Arabidopsis. *Plant Cell* 18: 412-421.

Dai, G.H., Nicole, M., Andary, C., Martinez, C., Bresson, E., Boher, B., et al. (1996) Flavonoids accumulate in cell walls, middle lamellae and callose-rich papillae during an incompatible interaction between *Xanthomonas campestris pv. malvacearum* and cotton. *Physiol. Mol. Plant Pathol.* 49: 285-306.

Denance, N., Sanchez-Vallet, A., Goffner, D. and Molina, A. (2013) Disease resistance or growth: the role of plant hormones in balancing immune responses and fitness costs. *Fr. Plant Sci.* 4: 155.

Dubos, C., Stracke, R., Grotewold, E., Weisshaar, B., Martin, C. and Lepiniec, L. (2010) MYB transcription factors in Arabidopsis. *Tr. Plant Sci.* 15: 573-581.

Fahlgren, N., Howell, M.D., Kasschau, K.D., Chapman, E.J., Sullivan, C.M., Cumbie, J.S., et al. (2007) High-Throughput Sequencing of Arabidopsis microRNAs: Evidence for Frequent Birth and Death of *MIRNA* Genes. *PLoS ONE* 2: e219.

Falcone Ferreyra, M.L., Rius, S.P. and Casati, P. (2012) Flavonoids: biosynthesis, biological functions, and biotechnological applications. *Fr. Plant Sci.* 3: 222.

Franco-Zorrilla, J.M., Valli, A., Todesco, M., Mateos, I., Puga, M.I., Rubio-Somoza, I., et al. (2007) Target mimicry provides a new mechanism for regulation of microRNA activity. *Nature Gen.* 39: 1033-1037.

Galeotti, F., Barile, E., Curir, P., Dolci, M. and Lanzotti, V. (2008) Flavonoids from carnation (*Dianthus caryophyllus*) and their antifungal activity. *Phytochem. Lett.* 1: 44-48.

Gamir, J., Pastor, V., Kaever, A., Cerezo, M. and Flors, V. (2014) Targeting novel chemical and constitutive primed metabolites against *Plectosphaerella cucumerina*. *Plant J.* 78: 227-240.

Gao, F., Wang, N., Li, H., Liu, J., Fu, C., Xiao, Z., et al. (2016) Identification of drought-responsive microRNAs and their targets in *Ammopiptanthus mongolicus* by using high-throughput sequencing. *Sci. Rep.* 6: 34601.

Glazebrook, J. (2005) Contrasting mechanisms of defense against biotrophic and necrotrophic pathogens. *Ann. Rev. Phytopathol.* 43: 205-227.

Guan, X., Pang, M., Nah, G., Shi, X., Ye, W., Stelli, D.M. and Chen, Z.J. (2014) miR828 and miR858 regulate homoeologous *MYB2* gene functions in Arabidopsis trichome and cotton fiber development. *Nat. Commun*. 5: 3050.

Jefferson, R.A., Kavanagh, T.A. and Bevan, M.W. (1987) GUS fusions: *beta-glucuronidase* as a sensitive and versatile gene fusion marker in higher plants. *EMBO J.* 6: 3901-3907.

Jeong, D.-H. and Green, P.J. (2013) The role of rice microRNAs in abiotic stress responses. *J. Plant Biol.* 56: 187-197.

Jones, J.D.G. and Dangl, J.L. (2006) The plant immune system. *Nature* 444: 323-329.

Liu, J., Osbourn, A. and Ma, P. (2015) MYB Transcription factors as regulators of phenylpropanoid metabolism in plants. *Mol. Plant* 8: 689-708.

Llave, C., Xie, Z., Kasschau, K.D. and Carrington, J.C. (2002) Cleavage of Scarecrow-like mRNA targets directed by a class of Arabidopsis miRNA. *Science* 297: 2053-2056.

Llorente, F., Alonso-Blanco, C., Sanchez-Rodriguez, C., Jorda, L. and Molina, A. (2005) ERECTA receptor-like kinase and heterotrimeric G protein from Arabidopsis are required for resistance to the necrotrophic fungus *Plectosphaerella cucumerina*. *Plant J.* 43: 165-180.

Mallory, A.C., Reinhart, B.J., Jones-Rhoades, M.W., Tang, G., Zamore, P.D., Barton, M.K., et al. (2004) MicroRNA control of *PHABULOSA* in leaf development: importance of pairing to the microRNA 5' region. *EMBO J.* 23: 3356-3364.

Mauch-Mani, B. and Slusarenko, A.J. (1994) Systemic acquired resistance in *Arabidopsis thaliana* induced by a predisposing infection with a pathogenic isolate of *Fusarium oxysporum*. *Mol. Plant Microbe Interact.* 7: 378-383.

Mehrtens, F., Kranz, H., Bednarek, P. and Weisshaar, B. (2005) The Arabidopsis transcription factor *MYB12* is a flavonol-specific regulator of phenylpropanoid biosynthesis. *Plant Physiol.* 138: 1083-1096.

Miedes, E., Vanholme, R., Boerjan, W. and Molina, A. (2014) The role of the secondary cell wall in plant resistance to pathogens. *Fr. Plant Sci.* 5: 358.

Molina, A., Goy, P.A., Fraile, A., Sánchez-Monge, R. and García-Olmedo, F. (1993a) Inhibition of bacterial and fungal plant pathogens by thionins of types I and II. *Plant Sci.* 92: 169-177.

Molina, A., Segura, A. and Garcia-Olmedo, F. (1993b) Lipid transfer proteins (nsLTPs) from barley and maize leaves are potent inhibitors of bacterial and fungal plant pathogens. *FEBS Lett.* 316: 119-122.

Naoumkina, M.A., Zhao, Q., Gallego-Giraldo, L., Dai, X., Zhao, P.X. and Dixon, R.A. (2010) Genome-wide analysis of phenylpropanoid defence pathways. *Mol. Plant Pathol.* 11: 829-846.

Navarro, L., Dunoyer, P., Jay, F., Arnold, B., Dharmasiri, N., Estelle, M., et al. (2006) A plant miRNA contributes to antibacterial resistance by repressing auxin signaling. *Science* 312: 436-439.

O'Connell, R., Herbert, C., Sreenivasaprasad, S., Khatib, M., Esquerre-Tugaye, M.T. and Dumas, B. (2004) A novel *Arabidopsis-Colletotrichum* pathosystem for the molecular dissection of plant-fungal interactions. *Mol. Plant Microbe Interact.*17: 272-282.

Palatnik, J.F., Allen, E., Wu, X., Schommer, C., Schwab, R., Carrington, J.C., et al. (2003) Control of leaf morphogenesis by microRNAs. *Nature* 425: 257-263.

Peer, W.A., Brown, D.E., Tague, B.W., Muday, G.K., Taiz, L. and Murphy, A.S. (2001) Flavonoid accumulation patterns of transparent *testa* mutants of Arabidopsis. *Plant Physiol.* 126: 536-548.

Piya, S., Kihm, C., Rice, J.H., Baum, T.J. and Hewezi, T (2017). Cooperative Regulatory Functions of miR858 and MYB83 during Cyst Nematode Parasitism. *Plant Physiol.* 174, 1897-1912.

Sharma, D., Tiwari, M., Pandey, A., Bhatia, C., Sharma, A. and Trivedi, P.K. (2016) MicroRNA858 is a potential regulator of phenylpropanoid pathway and plant development. *Plant Physiol.* 171: 944-959.

Soto-Suarez, M., Baldrich, P., Weigel, D., Rubio-Somoza, I. and San Segundo, B. (2017) The Arabidopsis miR396 mediates Pathogen-Associated Molecular Pattern-triggered immune responses against fungal pathogens. *Sci. Rep.* 7: 44898.

Staiger, D., Korneli, C., Lummer, M. and Navarro, L. (2013) Emerging role for RNA-based regulation in plant immunity. *New Phytol.* 197: 394-404.

Stracke, R., Ishihara, H., Huep, G., Barsch, A., Mehrtens, F., Niehaus, K., et al. (2007) Differential regulation of closely related *R2R3-MYB* transcription factors controls flavonol accumulation in different parts of the *Arabidopsis thaliana* seedling. *Plant J.* 50: 660-677.

Todesco, M., Rubio-Somoza, I., Paz-Ares, J. and Weigel, D. (2010) A collection of target mimics for comprehensive analysis of microRNA function in *Arabidopsis thaliana*. *PLoS Genet.* 6: e1001031.

van Loon, L.C., Rep, M. and Pieterse, C.M. (2006) Significance of inducible defense-related proteins in infected plants. *Ann. Rev. Phytopathol.* 44: 135-162.

Waki, T., Yoo, D., Fujino, N., Mameda, R., Denessiouk, K., Yamashita, S., et al. (2016) Identification of protein-protein interactions of isoflavonoid biosynthetic enzymes with 2-hydroxyisoflavanone synthase in soybean (*Glycine max* (L.) Merr.). *Biochem. Biophys. Res. Comm.* 469: 546-551.

Watkins, J.M., Hechler, P.J. and Muday, G.K. (2014) Ethylene-induced flavonol accumulation in guard cells suppresses reactive oxygen species and moderates stomatal aperture. *Plant Physiol.* 164: 1707-1717.

Weiberg, A., Wang, M., Bellinger, M. and Jin, H. (2014) Small RNAs: A new paradigm in plant-microbe interactions. *Ann. Rev. Phytopathol.* 52: 495-516.

Zipfel, C. (2014) Plant pattern-recognition receptors. *Tr. Immunol.* 35: 345-351.

Figure Legends

Fig. 1 Enhanced susceptibility of *MIR858* overexpressor plants to infection by the necrotrophic fungus *P. cucumerina* (A-D) or the hemibiotrophic fungus *C. higginsianum* (E-H). Three week-old plants were inoculated with fungal spores (1 x 10^5 spores/ml), or mock-inoculated. Three infection experiments, each with three independent *MIR858A* and *MIR858B* overexpressor lines (*MIR858A* OE and *MIR858B* OE; 24 plants per genotype) were carried out with similar results (results obtained with lines #1 and #2 are shown). Survival (C, F) and diseased leaf area (D, G) was determined at 15 dpi and 7dpi, respectively. Histograms show the mean ± SD. The statistical significance was determined by ANOVA (*, $P \leq 0.05$, **, $P \leq 0.01$, ***, $P \leq 0.001$). (**A)** Phenotype of *P.cucumerina*-infected *MIR858* plants. The *agb1.2* and *lin1* mutants were used as controls (susceptibility and resistance to *P. cucumerina*, respectively). Images show the phenotype at 7 days after inoculation with fungal spores. **(B)** Trypan blue staining of *P. cucumerina*-infected leaves was carried out at 72 hours post-inoculation (hpi). Bars represent 200 µm. **(C)** Survival of *P. cucumerina*-inoculated *MIR858* overexpressor plants. **(D)** Quantification of *P. cucumerina* DNA in fungal-inoculated wild-type, empty vector and *MIR858* overexpressor plants at 3 dpi as determined by real-time PCR using specific primers of *P. cucumerina β-tubulin* (values are fungal DNA levels normalized against the Arabidopsis *Ubiquitin21* gene). **(E)** Susceptibility of *MIR858A* overexpressor plants to infection by *C. higginsianum*. Dissected leaves of wild-type, empty vector and *MIR858A* OE plants at 7 dpi are shown. **(F, G)** Survival and diseased leaf area of *C. higginsianum*-inoculated *MIR858A* OE plants. (H) Quantification of *C. higginsianum* DNA in infected wild-type, empty vector and *MIR858* OE plants at 3 dpi as determined by real-time PCR using specific primers of *C. higginsianum ITS* region (values are fungal DNA levels normalized against the Arabidopsis *Ubiquitin21* gene).

Fig. 2 Resistance of *MIM858* plants to infection by the fungal pathogens *P. cucumerina* (A-D) or *C. higginsianum* (E-H). Plants were grown for three weeks and then inoculated with fungal spores (1 x 10^6 spores/ml) or mock-inoculated. Four independent *MIM858* lines were assayed (24 plants per genotype; results for lines #7, #10 and #14 are shown). Survival (B, F) and diseased leaf area (D, G) was quantified at 15 dpi and 7 dpi, respectively. Histograms show the mean ± SD of three biological replicates (ANOVA test, *, $P \leq 0.05$; **, $P \leq 0.01$; ***, $P \leq 0.001$). **(A)** Appearance of wild-type (WT, Col 0), empty vector (EV) and *MIM858* plants at 7 dpi after inoculation with *P. cucumerina* spores. The *agb1.2* and *lin1* mutants were used as controls (susceptibility and resistance to *P. cucumerina*, respectively). **(B)** Survival of *P. cucumerina*-inoculated *MIM858* and control plants. **(C)** Trypan blue staining of *P. cucumerina*-infected leaves of *MIM858* and control plants. Bars represent 200 µm. **(D)** Quantification of *P. cucumerina* DNA in wild-type, empty vector and *MIM858* plants at 3 dpi using specific primers of *P. cucumerina β-tubulin* relative to the Arabidopsis *Ubiquitin21* gene. **(E)** Resistance of *MIM858* plants to infection by *C. higginsianum*. Dissected leaves of wild-type, empty vector and MIM858 plants at 7 dpi are shown. **(F, G)** Survival and diseased leaf area of *C. higginsianum*-inoculated

MIM858 plants. **(H)** Quantification of *C. higginsianum* DNA in infected wild-type, empty vector and *MIM858* plants at 3 dpi as determined by real-time PCR using specific primers of *C. higginsianum ITS* region relative to the Arabidopsis *Ubiquitin21* gene).

Fig. 3 Expression of the defense related genes *PDF1.2* and *PR4* in *MIM858* (**A**) and *MIR858* overexpressor (**B**) plants in response to *P. cucumerina* infection. Three-week old plants were inoculated (+) with *P. cucumerina* spores (1×10^6 spores/ml) or mock-inoculated (-) (grey and black bars, respectively). Gene expression analyses were carried out by RT-qPCR at 3 days after inoculation. Histograms show the mean ± SD of one out 3 biological replicates, each with 24 plants per genotype, with similar results. Statistical significance was determined by ANOVA (***$P \leq 0.001$).

Fig. 4 Transcriptional regulation of *MIR858* induced by *P. cucumerina* in wild-type Arabidopsis plants. (**A-B)** Differential accumulation of pre-miR858 (left panel) and mature miR858 (right panel) in wild-type Arabidopsis (Col-0) plants treated with *P. cucumerina* spores (**A**) or elicitors (**B**) at the indicated times, as determined by RT-qPCR (pre-miR858) and stem-loop RT-qPCR (miR858) analysis. Values represent the mean fold change of pre-miR858 or miR858 in infected (**A**) or elicitor-treated (**B**) versus mock-treated samples based in three biological replicates per time point and log-scaled. Asterisks denote statistical differences in treated *vs* non-treated plants per each time point (ANOVA, *, $P \leq 0.05$; **, $P \leq 0.01$; n=3). **(C)** Histochemical analysis of GUS activity in *MIR858prom::GUS* plants that have been mock-inoculated or inoculated with *P. cucumerina* spores (24, 48 and 72 hours post-inoculation). As control, *prom35SCaMV::GUS* plants were used.

Fig. 5 Expression of genes involved in the early steps of the general phenylpropanoid biosynthesis pathway (*C4H*, *4CL* and *PAL4*) in *MIM858* (A) and *MIR858A* overexpressor (B) plants. RT-qPCR analysis was carried out using the *β-tubulin2* gene as the internal control. Histograms show the mean ± SD of 2 biological replicates, each with 24 plants per genotype. Statistical significance was determined by ANOVA (**, $P \leq 0.01$; ***, $P \leq 0.001$). C4H, Cinnamate-4-hydroxylase; PAL, phenylalanine ammonia-lyase; 4CL, 4-Coumarate-CoA Ligase.

Fig. 6 *In situ* flavonoid detection and antifungal activity of phenylpropanoid compounds in wild-type, *MIM858* and *MIR858* OE plants. **(A)** Flavonoid accumulation was visualized by DPBA staining of rosette leaves. Two week-old plants were inoculated with *P. cucumerina* spores (1×10^5 spores/ml), or mock-inoculated, and subjected to DPBA staining at 72 hours post-inoculation. **(B)** In vitro antifungal activity of the flavonoids naringenin and kaempferol, and the phenylpropanoid p-Coumaric acid against *P. cucumerina*. Fungal cultures were grown for 48h in PDB (potato dextrose broth) in the presence of increasing concentrations of the corresponding metabolite. Fungal growth is expressed as percentage of the growth of control cultures (100% growth represents fungal growth in control cultures). Two repeats of each bioassay were performed for each of two different preparations of spore suspensions.

Fig. 7 Lignin accumulation in wild-type, *MIM858* and *MIR858* OE plants was determined by whole-mount phloroglucinol staining. Pictures were taken at 72 hours post-inoculation with an Olympus DP71 camera. Bars represent 1 mm.

Supplementary data

Supplementary Fig. S1 Characterization of transgenic plants overexpressing *MIR858A* or *MIR858B*. **(A)** Accumulation of pre-miR858a and mature miR858a sequences in *MIR858* overexpressor (*MIR858A* OE, *MIR858B* OE) plants determined by RT-qPCR and stem-loop PCR, respectively. (B) Phenotype of plants that have been grown for 3 weeks under a 12h light/12h dark photoperiod condition. Two independent experiments were carried out with 3 independent lines for each genotype (at least 24 plants per line, each experiment). **(C)** Rosette leaf number and diameter (left and right panel, respectively). The rosette diameter (cm) was determined using Image J software (right panel). No significant differences were observed in leaf number between wild-type, *MIR858* overexpressor and wild type plants (ANOVA test).

Supplementary Fig. S2 Characterization of *MIM858* plants. (A) Accumulation of miR858a and miR858b in *MIM858* plants determined by stem-loop RT-qPCR. (B) Phenotype of *MIM858* plants that have been grown for 3 weeks under a 12h light/12h dark photoperiod condition. Two independent experiments were carried out with 3 independent *MIM858* lines (at least 24 plants per line, each experiment). **(C)** Rosette leaf number and diameter (left and right panel, respectively). The rosette diameter (cm) was determined using Image J software (right panel). No significant differences were observed in leaf number between wild-type, *MIM858* and wild type plants (ANOVA test).

Supplementary Fig. S3 Dissected leaves of three-week-old *MIM858* and control plants that have been mock-inoculated or inoculated with *P. cucumerina* spores (1×10^6 spores/ml). Pictures were taken at 7 days post-inoculation.

Supplementary Fig. S4 Resistance of *MIM858* plants to infection by the hemibiotrophic fungal pathogen *Fusarium oxysporum* f. sp. *conglutinans* (*FOC*). Plants were grown for 3 weeks and then inoculated with a suspension of FOC spores (1×10^6 spores/ml). **(A)** Rosette leaves *MIM858*, wild-type and empty vector plants at 15 days after inoculation with *FOC*. **(B, C)** Survival (B) and leaf area with disease symptoms (C) was recorded at 30 dpi and 15 dpi, respectively. **(D)** Quantification of fungal DNA in leaves of *FOC*-inoculated plants was carried out by qPCR at 10 dpi relative to the Arabidopsis *Ubiquitin21* gene.

Supplementary Fig. S5. Expression of *PDF1.2*, *PR4*, *VSP2* and *LOX2* in *MIM858* (**A**) and *MIR858* overexpressor (**B**) plants in response to *P. cucumerina* infection. Three-week old plants were inoculated (+) with *P. cucumerina* spores (1×10^6 spores/ml) or mock-inoculated (-) (grey and black bars, respectively). Gene expression analyses were carried out by RT-qPCR at 3 days after inoculation. Histograms show the mean ± SD of one out 3 biological replicates, each with 24 plants per genotype, with similar results. Statistical significance was determined by ANOVA (***$P \leq 0.001$).

Supplementary Fig. S6 Fluorimetric analysis of GUS activity in *MIR858prom::GUS* plants that have been mock-inoculated or inoculated with *P. cucumerina* spores (72 hours post-inoculation). As control, *prom35SCaMV::GUS* plants were used. $P \leq 0.01$ (ANOVA test).

Supplementary Fig. S7 Expression analysis of *MYB* transcription factor genes regulated by miR858 in *MIM858* and *MIR858A* overexpressor plants (A, B) in response to infection by *P. cucumerina* (C). RT-qPCR analysis was carried out using the *β-tubulin2* gene as the internal control. Histograms show the mean ± SD of 2 biological replicates, each with 24 plants per genotype. Statistical significance was determined by ANOVA (*, $P \leq 0.05$; ***, $P \leq 0.001$). (A) Accumulation of miR858 target genes (*AtMYB11*, *AtMYB12*, *AtMYB111*, *AtMYB13* and *AtMYB20*) in *MIM858* plants. *AtMYB11*, *AtMYB12* and *AtMYB111* are involved in phytoalexin biosynthesis. These three genes were further analyzed in (B) *MIR858A* overexpressor plants and in (C) wild-type plants mock-inoculated (-) and inoculated with *P. cucumerina* (+) at 72 hpi.

Supplementary Fig. S8 Expression analysis of phenylalanine ammonia-lyase (*PAL*) genes in *MIM858* and *MIR858A* overexpressor plants. Accumulation of *PAL1, PAL2* and PAL3 transcripts was determined by RT-qPCR analysis in *MIM858* (A) and *MIR858A* overexpressor (B) plants. The *β-tubulin2* gene was used as the internal control. Statistical significance was determined by ANOVA (**, $P \leq 0.01$; ***, $P \leq 0.001$).

Supplementary Fig. S9 Differences in morphology of hyphae in *P. cucumerina* cultures grown in PDB medium (Control) and in the presence of kaempferol (4 mM), naringenin (2 mM) or p-Coumaric acid (1 mM). Micrographs were taken after 48 h of incubation. Bioassays were carried out 3 times with different preparations of spore suspensions.

Supplementary Fig. S10 RT-qPCR analysis of *CAD5* and *CAD6* expression in *MIM858* plants. The *β-tubulin2* gene was used as the internal control. Histograms show the mean ± SD of 2 biological replicates, each with 24 plants per genotype. Statistical significance was determined by ANOVA (***, $P \leq 0.001$).

Supplementary Table S1 Sequences of oligonucleotides used in this study.

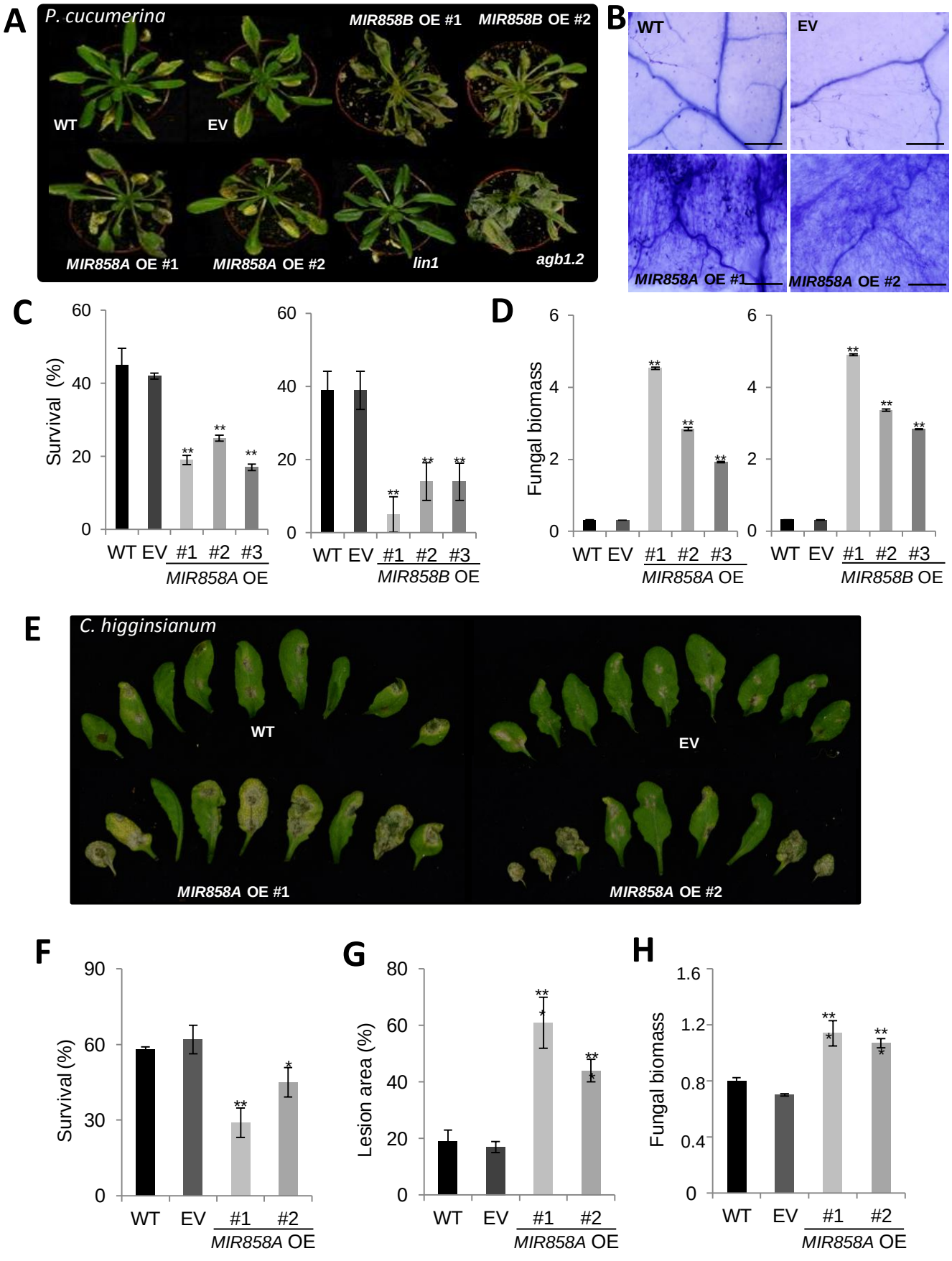
A
P. cucumerina
MIR858B OE #1
MIR858B OE #2
WT
EV
MIR858A OE #1
MIR858A OE #2
lin1
agb1.2
B
WT
EV
MIR858A OE #1
MIR858A OE #2
C
Survival (%)
WT EV #1 #2 #3
MIR858A OE
MIR858B OE
D
Fungal biomass
E
C. higginsianum
WT
EV
MIR858A OE #1
MIR858A OE #2
F
Survival (%)
G
Lesion area (%)
H
Fungal biomass

Figure 1

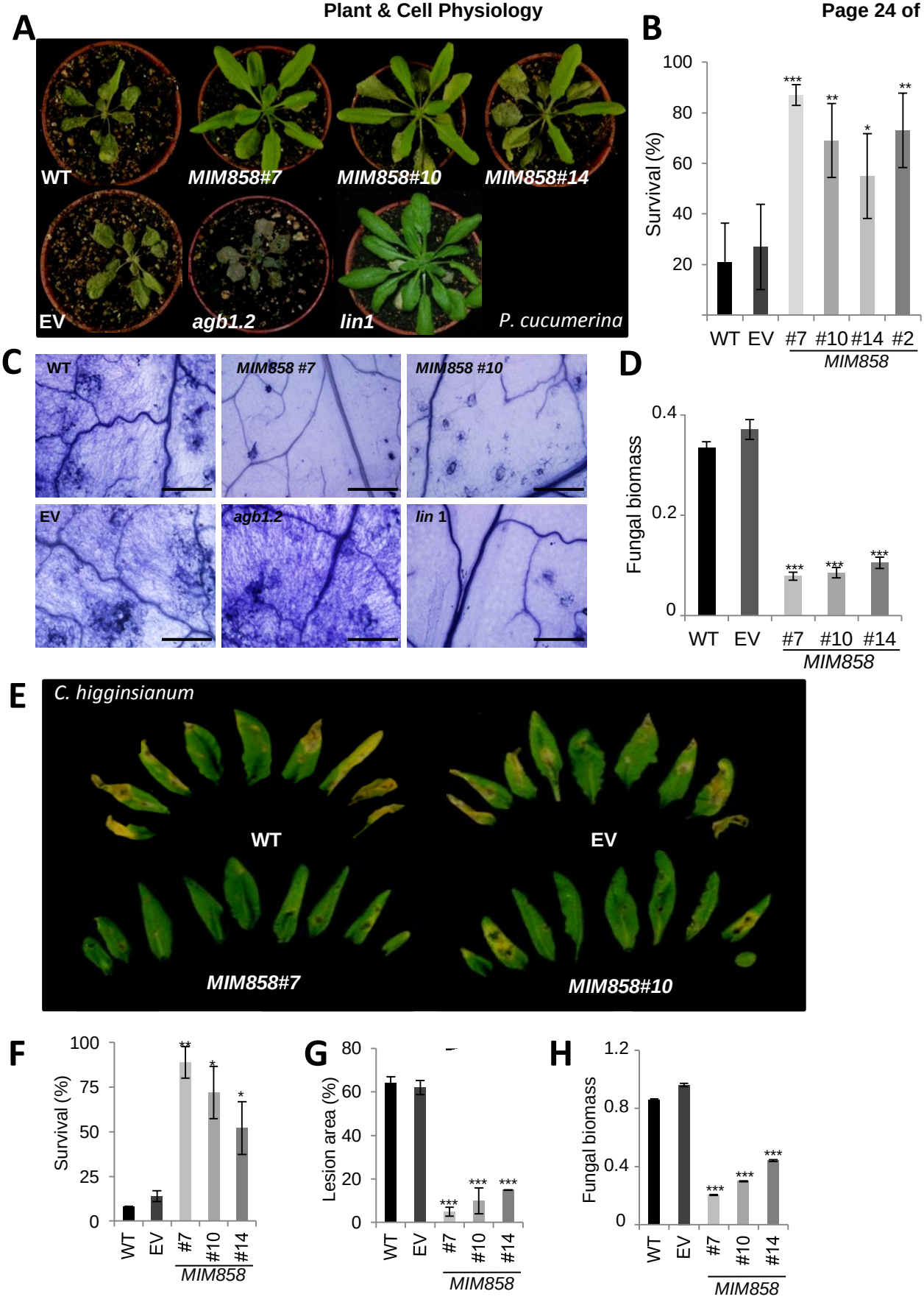
A
WT
MIM858#7
MIM858#10
MIM858#14
EV
agb1.2
lin1
P. cucumerina
B
Survival (%)
WT EV #7 #10 #14 #2
MIM858
C
WT
MIM858 #7
MIM858 #10
EV
agb1.2
lin 1
D
Fungal biomass
WT EV #7 #10 #14
MIM858
E
C. higginsianum
WT
EV
MIM858#7
MIM858#10
F
Survival (%)
WT EV #7 #10 #14
MIM858
G
Lesion area (%)
WT EV #7 #10 #14
MIM858
H
Fungal biomass
WT EV #7 #10 #14
MIM858

Figure 2

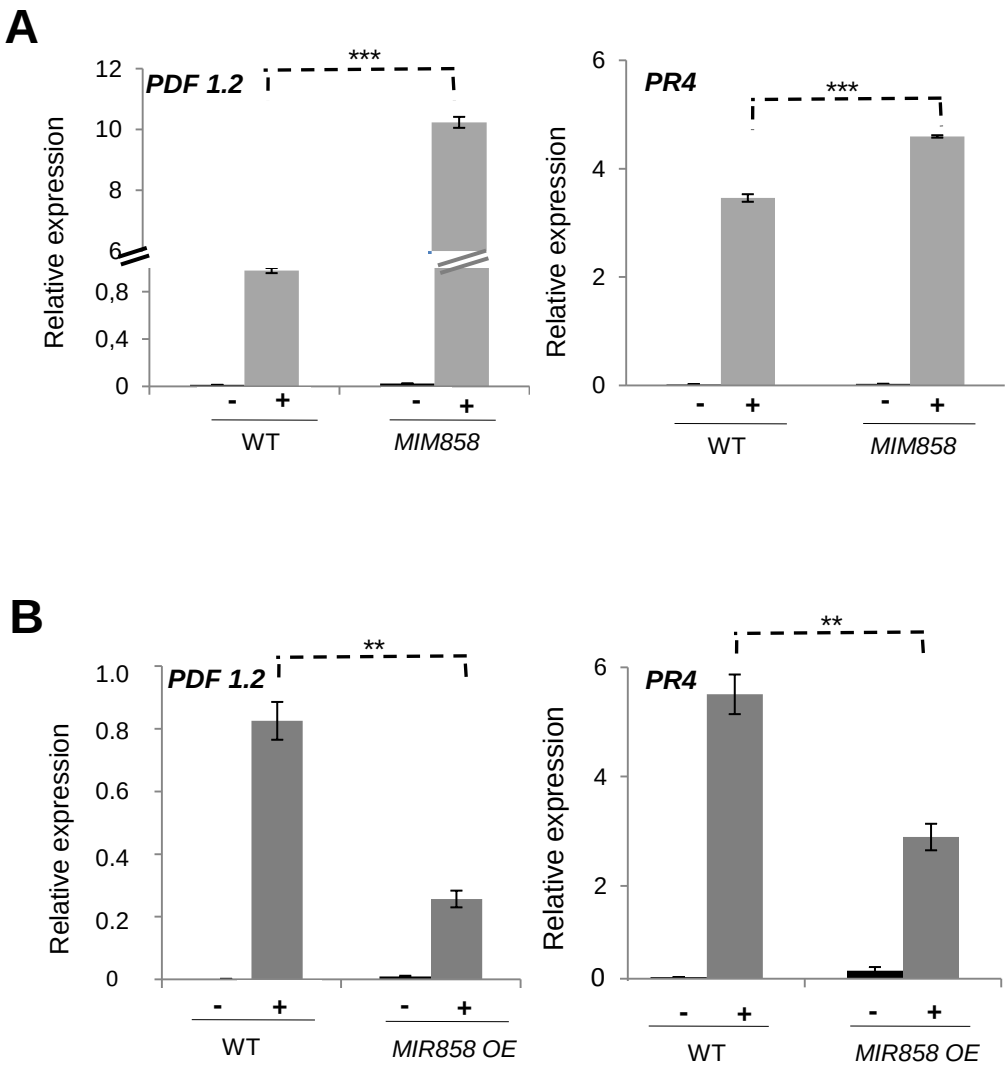
A
PDF 1.2
***
Relative expression
12
10
8
6
0,8
0,4
0
- + - +
WT
MIM858
PR4
***
Relative expression
6
4
2
0
- + - +
WT
MIM858
B
PDF 1.2
**
Relative expression
1.0
0.8
0.6
0.4
0.2
0
- + - +
WT
MIR858 OE
PR4
**
Relative expression
6
4
2
0
- + - +
WT
MIR858 OE

Figure 3

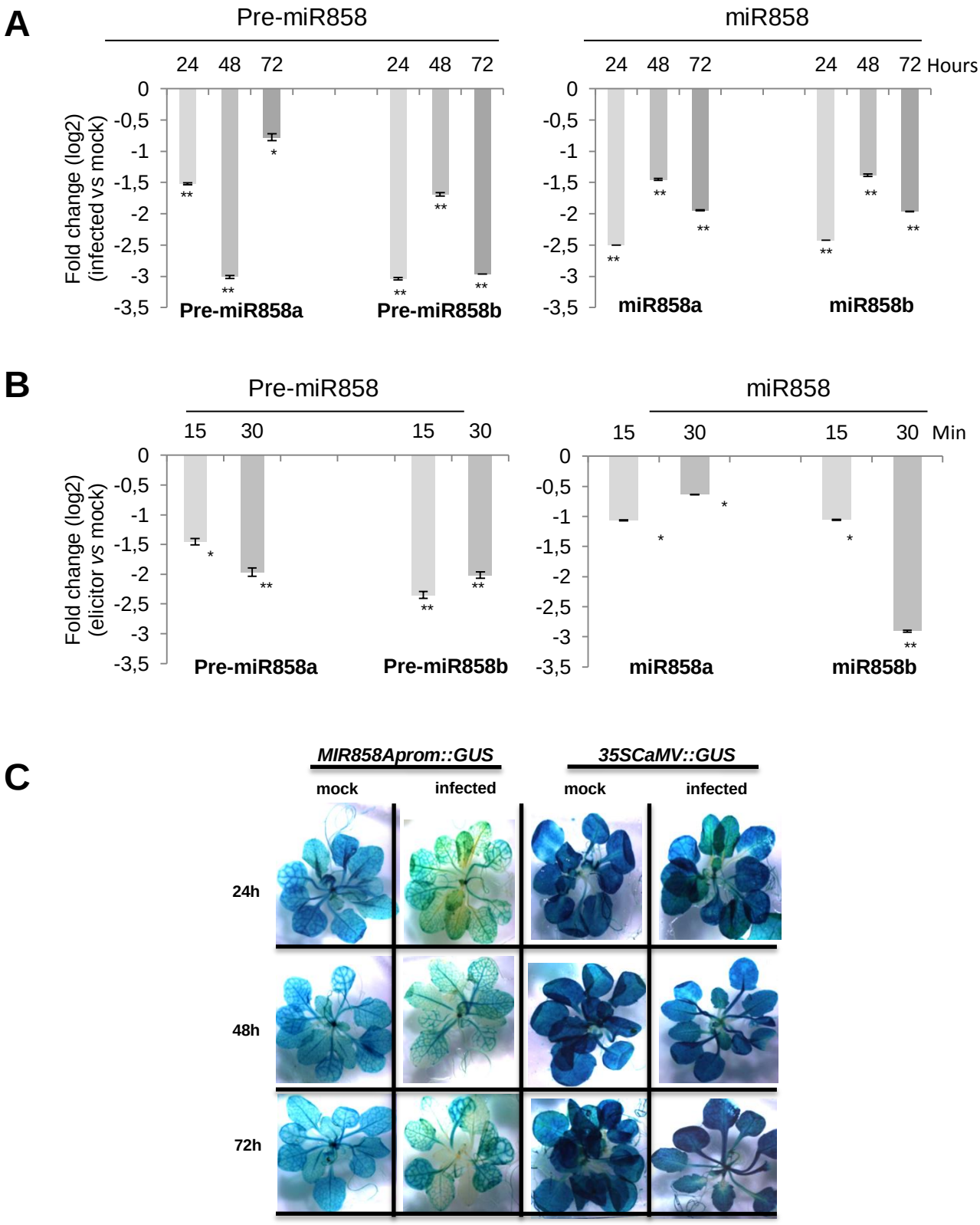
A
Pre-miR858
miR858
24 48 72 24 48 72 Hours
Fold change (log2) (infected vs mock)
0 -0,5 -1 -1,5 -2 -2,5 -3 -3,5
Pre-miR858a
Pre-miR858b
miR858a
miR858b
B
Pre-miR858
miR858
15 30 15 30 Min
Fold change (log2) (elicitor vs mock)
Pre-miR858a
Pre-miR858b
miR858a
miR858b
C
MIR858Aprom::GUS
35SCaMV::GUS
mock
infected
mock
infected
24h
48h
72h

Figure 4

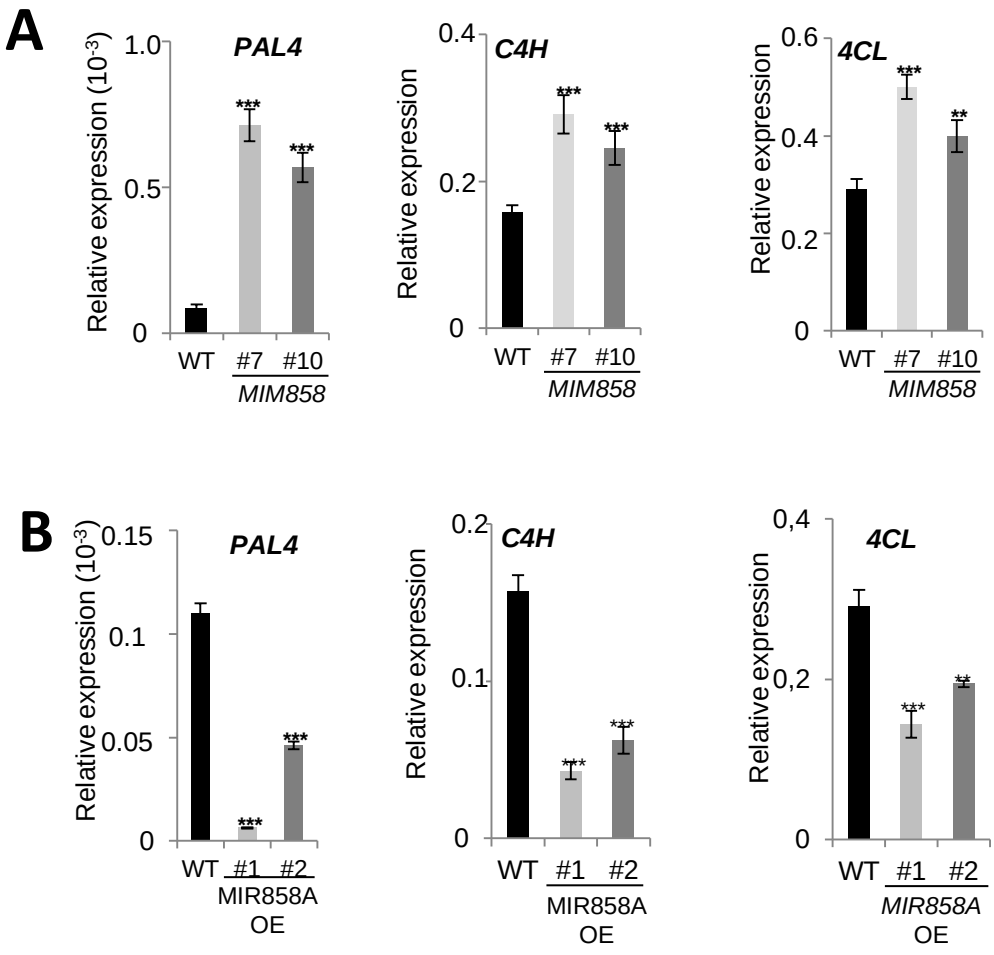
A
PAL4
C4H
4CL
Relative expression (10-3)
Relative expression
1.0
0.5
0
0.4
0.2
0.6
WT
#7
#10
MIM858
B
0.15
0.1
0.05
0.2
0,4
0,2
#1
#2
MIR858A OE
MIR858A OE

Figure 5

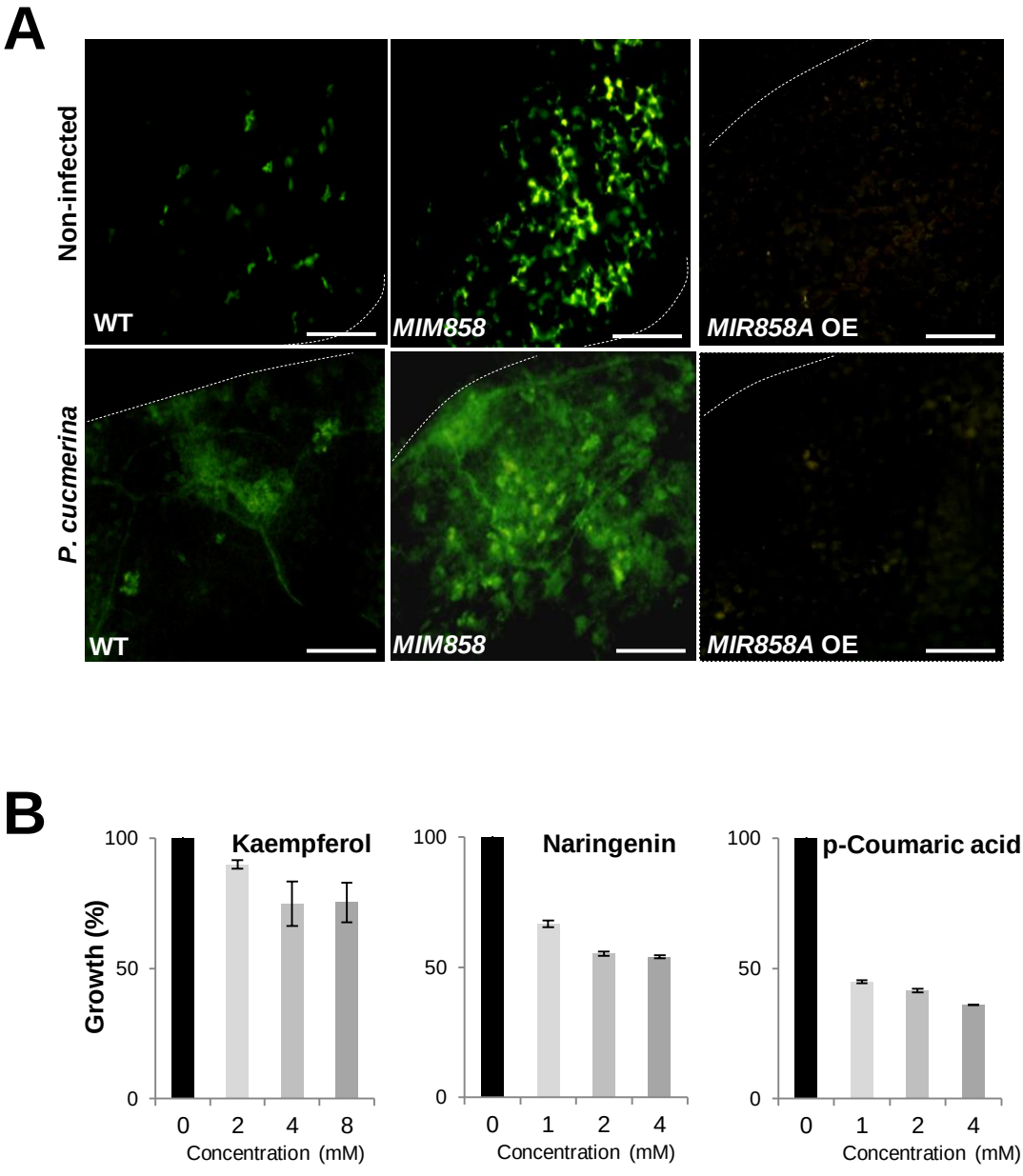
A
Non-infected
P. cucmerina
WT
MIM858
MIR858A OE
WT
MIM858
MIR858A OE
B
Kaempferol
Naringenin
p-Coumaric acid
Growth (%)
100
50
0
0 2 4 8
0 1 2 4
Concentration (mM)

Figure 6

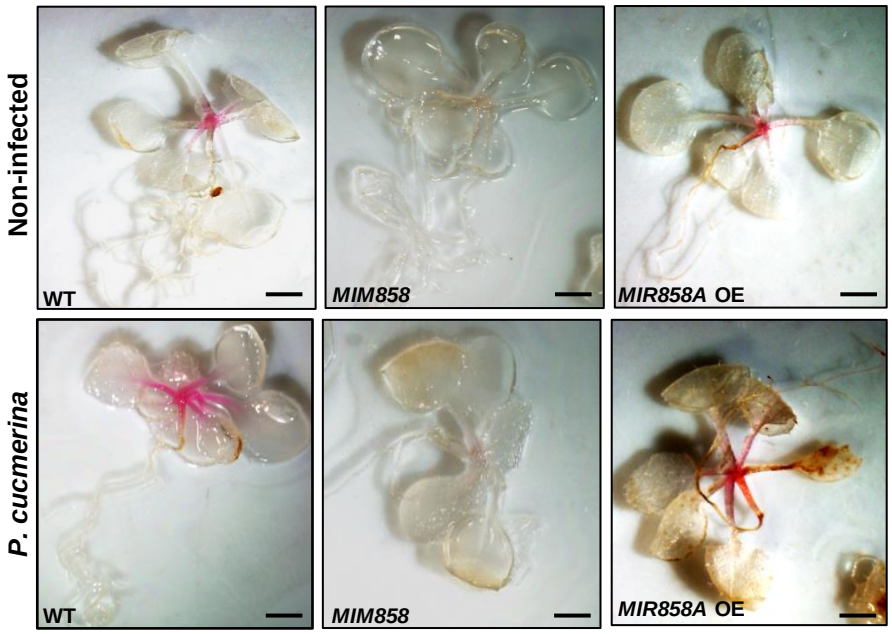
Non-infected
P. cucmerina
WT
MIM858
MIR858A OE
WT
MIM858
MIR858A OE

Figure 7